



Analytical characterisation and corrosion behaviour of bis-[triethoxysilylpropyl]tetrasulphide pre-treated AA2024-T3

A. Cabral ^{a,b}, R.G. Duarte ^b, M.F. Montemor ^b,
M.L. Zheludkevich ^c, M.G.S. Ferreira ^{b,c,*}

^a *Instituto Superior de Engenharia de Lisboa, Rua Conselheiro Emídio Navarro, 1-1950-062 Lisboa, Portugal*

^b *Instituto Superior Técnico, ICEMS, Department of Chemical Engineering, Avenue Rovisco Pais 1049-001 Lisboa, Portugal*

^c *Department of Ceramics and Glass Engineering, University of Aveiro, 3810-193, Aveiro, Portugal*

Available online 22 September 2004

Abstract

This work aims at studying the corrosion behaviour of AA2024-T3 pre-treated with bis-[triethoxysilylpropyl]tetrasulphide. Simultaneously, the work investigates the influence of the Cu-rich intermetallic particles on the formation of the silane film. The analytical characterisation of the silane films was performed by Auger electron spectroscopy and X-ray photoelectron spectroscopy. The corrosion performance of the pre-treated substrates was evaluated by electrochemical impedance spectroscopy. Atomic force microscopy associated with Kelvin probe was also used to determine the influence of the silane film on the Volta potential distribution on the alloy surface. The results show that copper present in the intermetallics plays an important role on the film formation.

© 2004 Elsevier Ltd. All rights reserved.

* Corresponding author. Address: Department of Ceramics and Glass Engineering, University of Aveiro, 3810-193, Aveiro, Portugal. Tel.: +351 234 370354/218 417234; fax: +351 234 425300/218 404589. E-mail address: mgferreira@cv.ua.pt (M.G.S. Ferreira).

Keywords: AA2024-T3; B. EIS; B. XPS; B. AFM; Surface pre-treatment; Silanes

1. Introduction

Silane pre-treatments are considered as environmental friendly replacements for the existing Cr(VI)-based processes. Recently, pre-treatments based on the use of silanes attracted the attention of many industries because silanes are known as good coupling agents, conferring in addition, corrosion protection [1–8]. Moreover they seem to comply with environmental issues.

Organofunctional silanes are hybrid organic–inorganic compounds. They can act as coupling compounds across organic–inorganic interfaces, if they are used properly. Functional silanes have a $X_3Si(CH_2)_nY$ type of structure, where X represents a hydrolysable group such as methoxy or ethoxy and Y a functional group such as amine, epoxy or mercapto, which is not hydrolysable. The functional group can attach to the paint polymer, which is applied on the silane-treated metal. When the silane is symmetrical relative to the functional group, Y, i.e., if there are two hydrolysable X_3 groups, these molecules are known as bis-functional silanes, having the structure $X_3Si(CH_2)_nY(CH_2)_nSiX_3$. The bis-sulphur silane is one of these molecules, where Y is the sulphur group (S_{3-4}). Bis-functional silanes could act as good corrosion protection agents. They are able to form a high density of Me–O–Si bonds at the interface although these bonds can be hydrolysed by a large amount of water. To prevent hydrolysis of these bonds, it is necessary to reduce water uptake in the film. The formation of a cross-linked structure, which reduces the film porosity, is one of the ways that enhances the resistance against water uptake. The establishment of hydrophobic Si–O–Si bonds also prevents water uptake. Moreover, in the case of the bis-sulphur silane films, the sulphur chains also help to increase film hydrophobicity. Therefore, water permeation will be very difficult in such cross-linked silane coatings and good corrosion protection of the metal can be achieved [6]. In recent works [7] it was reported that the bis-sulphur silanes could also form sulphides by reacting with metals with a high affinity for S, such as Cu, Ni and Zn.

Van Ooij et al. [8] studied several silane-coupling agents on polished zinc and phosphated electrogalvanized steel substrates. The main conclusion of these works is that the performance of silane coupling agents used as primers on galvanised steel strongly depends on the surface composition of the metallic substrate. Other works report that the control of parameters such as concentration and pH of the silane solution and curing procedure are very important in the formation of the protective silane films [9].

Recently, studies concerned with the use of bis-[triethoxysilylpropyl]tetrasulphide (BTESPT), $(C_2H_5O)_3Si-(CH_2)_3-S_x-(CH_2)_3-Si(OC_2H_5)_3$ which has an average x value of 3.8 and bis-amino silanes have been published [1,6,7]. BTESPT was tested with good results on Al alloys, Zn–Ni coated steel and galvanised steel. In the case of the AA2024-T3 the pre-treatment with BTESPT can reduce the dissolution of the

Al matrix surrounding the Al₂CuMg particles [10]. Results of several tests including ASTM B 117 salt spray tests [3] showed that metals treated with BTESPT exhibit good corrosion performance.

In the present work, results on the corrosion resistance of AA2024-T3 pre-treated with the bis-sulphur silane (BTESPT) are presented. Some details on the mechanism of film formation are also discussed. To perform the present study Auger electron spectroscopy (AES), X-ray photoelectron spectroscopy (XPS), scanning Kelvin probe microscopy (SKPFM) and electrochemical impedance spectroscopy (EIS) were used.

2. Experimental

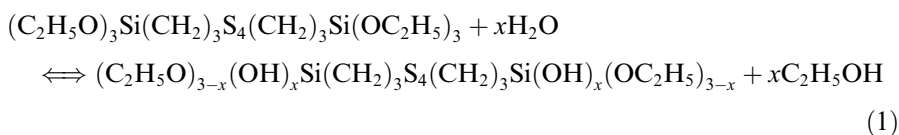
2.1. Preparation of the metallic substrates

AA2024-T3 and pure aluminium (99.999%) panels were ultrasonically degreased with acetone, alkaline cleaned by immersion for 5 min at 40 °C in 30 g/l aqueous solution of TURCOTM 4215 (TURCOTM product) followed by dismutting for 4 min at room temperature in a solution of DEOXIDISERTM 1 (Amchem product).

Samples for Auger, XPS and SKPFM analysis were polished down to 1 μm diamond paste before the cleaning procedure.

2.2. Pre-treatment

The 4% BTESPT solution was prepared by dissolving the correct volume of silane in a mixture of methanol and deionised water: silane/DI water/methanol = 4/5.5/90.5 vol%. The BTESPT solution was stabilized for at least 4 days before use, allowing it to attain a high degree of hydrolysis, according to reaction (1):



AA2024-T3 panels were immersed in the BTESPT solution for 1 s. The treated panels were then removed from the solution and dried by blowing air and cured at 120 °C for 40 min. Samples of pure copper and of pure aluminium were also treated with the BTESPT solution for 1 s for comparison with AA2024-T3.

A standard commercial Cr(VI)-based pre-treatment (TURCOTM Accelagold) was used as reference.

Electrochemical studies were performed during immersion in 0.1 N NaCl solution.

2.3. Measurements

The EIS measurements were carried out using a Gamry FAS1 Femtostat + PC4 Controller Board and all the measurements were performed at room temperature

in a Faraday cage. A three-electrode arrangement was used. A saturated calomel electrode was used as reference and a platinum wire was used as counter electrode. The measuring frequency ranged from 10^5 Hz to 10^{-3} Hz. All EIS spectra were recorded after ~ 10 min of immersion in the electrolyte at the open circuit potential. At least two measurements were performed for each condition.

AES depth profiles, Auger mapping and XPS analysis were carried out using a Scanning Auger Microprobe (VG Scientific) equipped with a field emission type electron gun, a concentric hemispherical analyser and a differentially pumped ion gun. Auger spectra were taken using a 10 keV, 40 nA primary electron beam, making an angle of 30° with the surface. XPS was performed using a Mg (non-monochromated) anode.

Scanning Kelvin probe force microscopy (SKPFM) was performed with a commercial AFM (Nanoscope Digital Instruments NanoScope III system) in the tapping mode. This technique was used to produce maps of the Volta potential distribution over the surface of the AA2024-T3 in air, before and after treatment with the silane. The technique provides features regarding shape, position, compositional heterogeneities and local potential values of the intermetallic compounds with submicrometer resolution [11–14]. For accurate measurements a SiO_2 grid pattern consisting of an array of square openings was created on the specimen surface. The grid served as a reference register so that the same location could be measured before and after the silane deposition. The size of the squares on the SiO_2 mask was $50 \times 50 \mu\text{m}$. The SiO_2 mask, with a thickness of 100 nm, was deposited with a Electrotech Delta plasma enhanced chemical vapour deposition. To etch the SiO_2 layer a LAM Research reactive ion etching was used. The mask pattern was defined photolithographically using a laser direct write system (HIMT-DWLii) with a HeCd laser on positive photoresist.

3. Results and discussion

3.1. Auger and XPS results

The XPS analysis performed on pure aluminium pre-treated with BTESPT showed the presence of an Al 2p ionisation composed by two peaks: one at 72.08 eV, which is characteristic of metallic Al and another one at 74.72 eV, which is the result of a mixture of Al oxides and hydroxides (Fig. 1). The presence of metallic aluminium suggests that the silane film does not cover the entire surface. For the AA2024-T3, before treatment, the XPS analysis clearly showed the presence of copper, as expected, since the amount of this element in the alloy composition is around 4%. After the pre-treatment with the silane it was not possible to detect the Al 2p and Cu 2p ionisations, suggesting that a homogeneous film was formed on the surface. The S2p ionisations showed two peaks around 164 eV (S2p_{3/2}) and 165 eV (S2p_{1/2}) (Fig. 2a). These peaks can be attributed to the C–S bonds. The binding energy of Si2p ionisation (~ 103 eV) is characteristic of the presence of Si–O bonds (Fig. 2b).

The comparison of the atomic % of silicon and sulphur for the AA2024-T3 alloy and for the pure aluminium shows a significantly lower content of these elements on

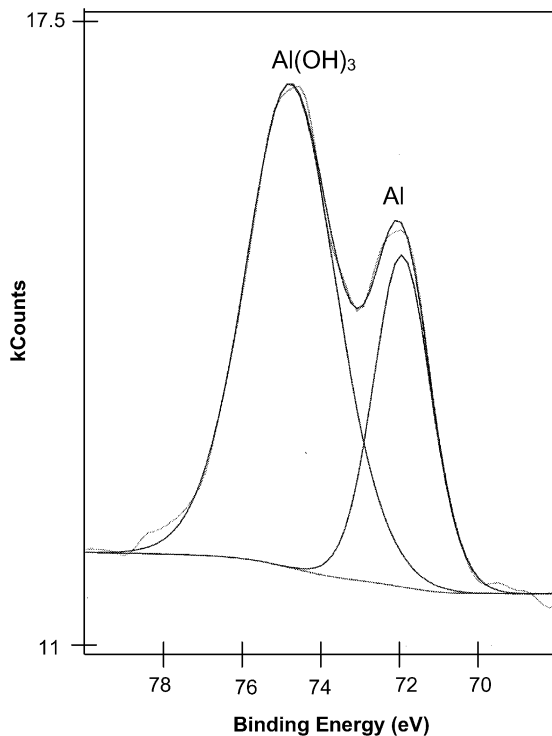


Fig. 1. Al 2p ionisation obtained on pure aluminium treated with BTESPT.

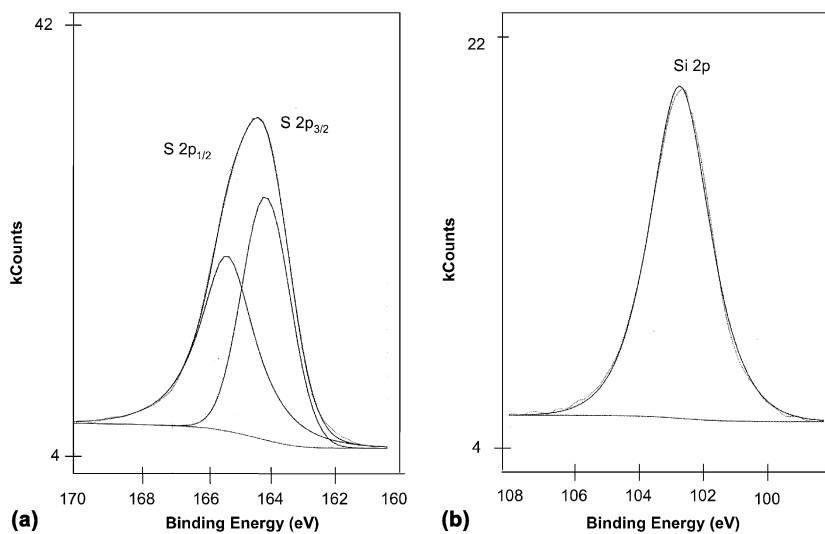


Fig. 2. (a) S2p and (b) Si2p ionisations obtained on AA2024-T3 treated with BTESPT.

Table 1

Composition of the surface determined by XPS for pure aluminium, AA2024-T3 and copper (all treated with silane)

Element	Al 99.999%	AA2024-T3	Copper
Si-O	10.4	21.0	22.4
S-C	7.1	26.9	28.1
C-O/S	13.4	8.7	5.8
C-Hn	41.1	25.7	23.4

the surface of pure aluminium (Table 1). The above results suggest that the formation of the film seems to be facilitated on the alloy surface. Since the main difference between the Al alloy and pure aluminium is the presence of intermetallics, most of them containing copper, it is plausible to think that these intermetallics may help in the formation of the silane film. In fact, the results depicted in Table 1 for copper samples treated with BTESPT suggest that there is a good affinity between the silane and copper.

The AES depth profiles obtained on AA2024-T3 (Fig. 3) reveal the presence of a silane film deposited upon the aluminium oxide. The silicon content starts to decrease after ~50s of etching, and vanishes after ~150s, as consequence of the removal of the outermost silane molecules. An interesting feature is the evolution of the sulphur content with the depth. Sulphur remains on the surface until a depth that is almost twice that of silicon. Thus, silicon groups are firstly removed, whereas sulphur groups remain attached to the surface.

The Auger depth profiles obtained for the silane films formed on the AA 2024-T3 treated with BTESPT for different dipping times, were identical, suggesting that the film thickness is not affected by the pre-treatment time. It is well accepted that silanol groups, formed during hydrolysis in the water/alcohol solution, are adsorbed by the

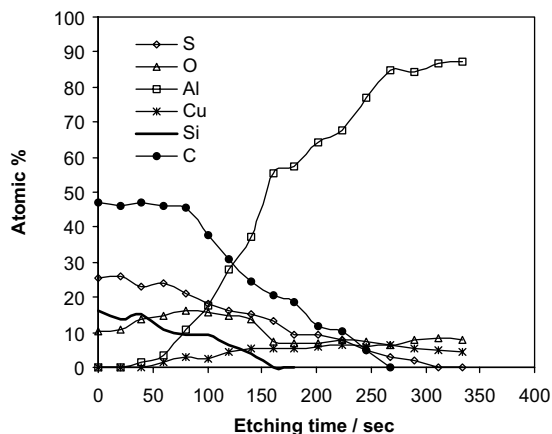


Fig. 3. Auger depth profiles for the film formed on AA2024-T3.

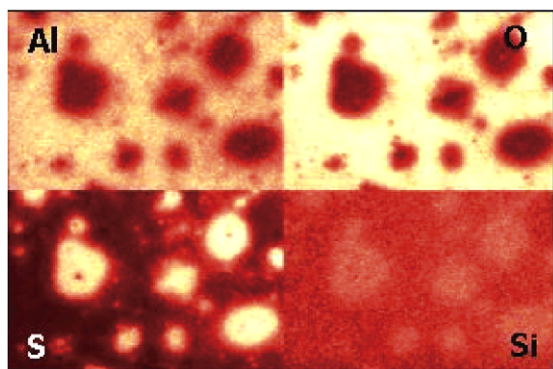


Fig. 4. Auger map obtained on AA2024-T3 surface treated with BTESPT after 100s of etching.

high-energy metal oxides of the native surfaces, forming hydrogen bonds. Upon curing, such bonds seem to be replaced by metallosiloxane bonds, ($-\text{Me}-\text{O}-\text{Si}$). The remaining silanol groups in the outer layers of the film will condense and form $\text{Si}-\text{O}-\text{Si}$ bonds [3]. Thus, during the first instants of contact with the silane solution, the native oxide/hydroxide surface is immediately covered with hydrolysed silane molecules and no more bonds are established for longer contact times.

The spatial distribution of the different elements on the surface of AA2024-T3 pre-treated with BTESPT after 100s of etching (enough to remove silicon) was examined by scanning Auger mapping (Fig. 4). In these maps the darkest areas correspond to a very low content of the element under study, whereas the brightest areas correspond to the highest contents of the element. The figure shows “islands” of sulphur that remain on the surface even after most of the silicon has been removed. It is also possible to observe that the sulphur rich-areas are coincident with the Cu-rich intermetallic particles (dark zones in the Al and O maps). The surrounding surface is, in contrast, richer in aluminium and oxygen, and very poor in sulphur.

3.2. EIS results

Figs. 5 and 6 depict the impedance Bode plots obtained for the AA2024-T3 and for the same alloy pre-treated either with BTESPT or with a Cr(VI)-based solution, after 10 min and 24 h of immersion in 0.1 N NaCl solutions, respectively. In these plots the impedance at the lowest frequencies can be correlated with the corrosion resistance of the system. Thus, higher impedances values account for enhanced corrosion protection. The impedance spectra show that the pre-treatment with BTESPT provides higher impedance values comparatively to the untreated alloy and to the commercial chromate conversion coating. This effect can be the result of a decrease on the rate of the corrosion reaction in the presence of the silane film and/or a barrier effect that enhances the protection of the natural oxide film.

The phase angle plots show some changes occurring during exposure to the NaCl solutions. To understand these changes the impedance plots obtained for

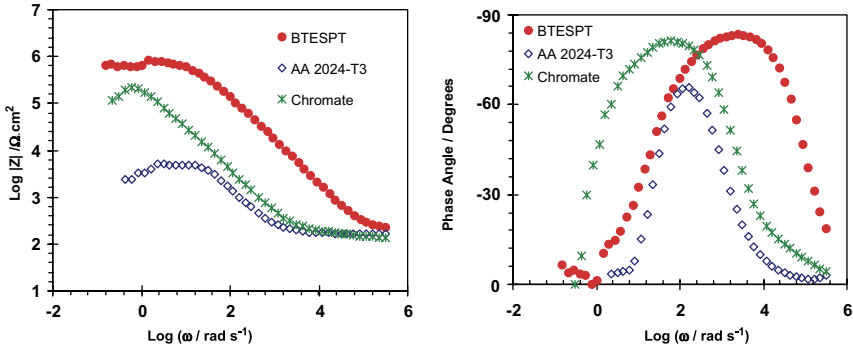


Fig. 5. EIS Bode plots obtained for AA2024-T3 immersed in 0.1N NaCl, during 10min.

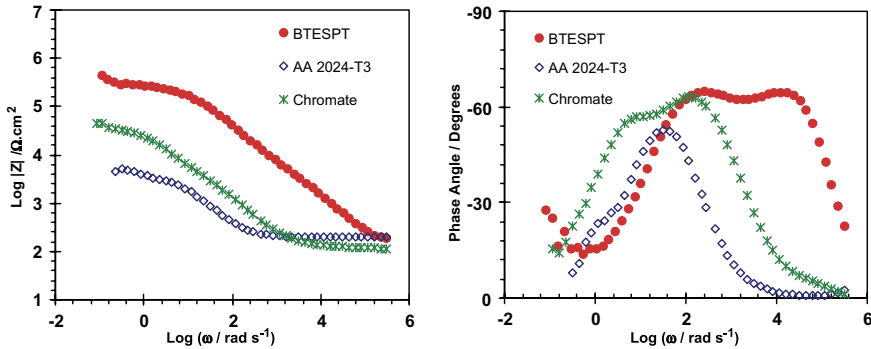


Fig. 6. EIS Bode plots obtained for AA2024-T3 immersed in 0.1N NaCl, during 24h.

the BTESPT pre-treated alloy were fitted using the equivalent circuit depicted in Fig. 7, which have also been used by other authors [6]. The equivalent circuit used in the simulation of the experimental results includes three time constants: one describing the behaviour of the system at high frequencies, which is associated with the presence of the silane film; another at around 10^2 rad/s, accounting for the presence of an intermediate layer between the outermost silane film and the substrate and, a third one, in the lowest frequency range associated with corrosion onset. The results were fitted using CPE's (constant phase element) that give an approximate value of the capacitance (if $n \approx 1$). The fitting results are depicted in Figs. 8 and 9.

The EIS spectra obtained for the BTESPT pre-treated alloy after 10min do not yet evidence the lowest frequency time constant, since corrosion has not started. Thus, the association CPE(corr)/R(corr) was not considered in the fitting of the results depicted in Fig. 8. However, it was included in the fitting of the EIS spectra obtained after 24h—Fig. 9.

After 10min of immersion the capacitance of the outermost silane film is 7.6×10^{-8} F/cm² and slightly increases with time, reaching a value of 1.4×10^{-7} F/cm²

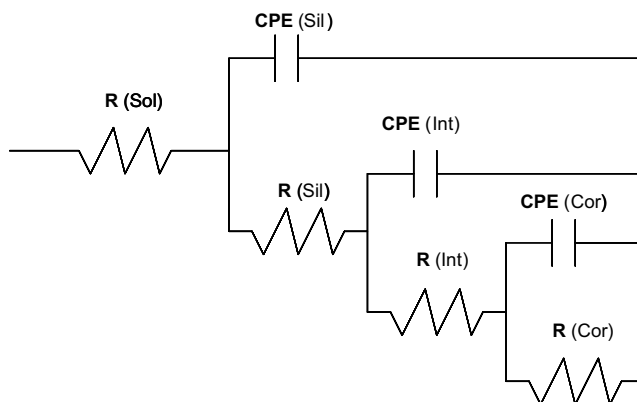


Fig. 7. Electrical equivalent circuits used for numerical simulation of the EIS results obtained on BTESPT pre-treated AA2024-T3.

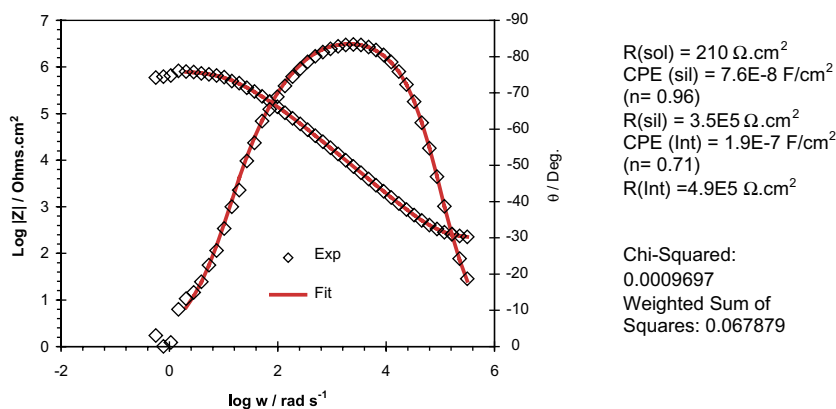


Fig. 8. Fitted and experimental EIS plots for BTESPT pre-treated AA2024-T3 (10 min of immersion in neutral 0.1 N NaCl solution).

after 24h of immersion. Simultaneously, the film resistance decreases by about two orders of magnitude. These changes are associated with water uptake by the silane film.

The time constant observed in the intermediate frequency range becomes more defined with time. Initially, the capacitance associated with this feature is around $2 \times 10^{-7} F/cm^2$ and increases with time, although remaining in the same order of magnitude. The resistance shows an identical trend, but in the opposite direction. Other authors [3,6,7] also observed the presence of this feature, which was assigned to a phase between the outermost silane film layers and the native aluminium oxide. Similar features were also reported for galvanised steel pre-treated with BTESPT [15]. Such phase can result from the formation of stable Si–O–Al and/or Si–O–Si

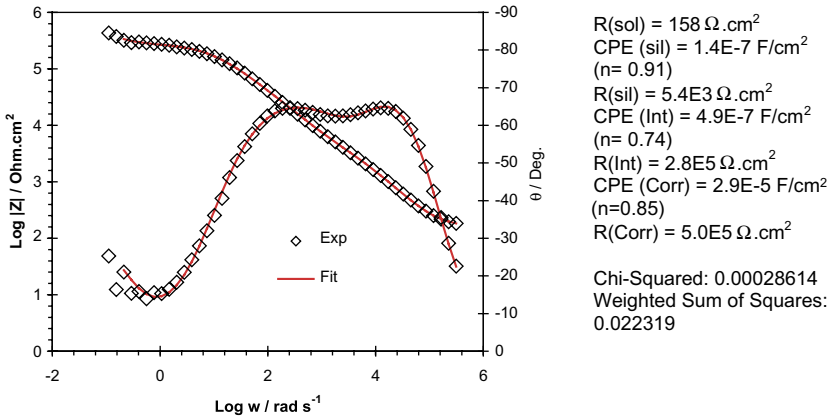
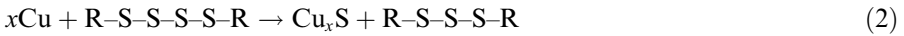


Fig. 9. Fitted and experimental EIS plots for BTESPT pre-treated AA2024-T3 (24h of immersion in neutral 0.1N NaCl solution).

bonds. However, it seems to include the products resulting from the reaction of the Cu-rich intermetallics with the bis-sulphur silane, according to [6]:



The breakdown of the sulphur bridges of the silane molecules on the sulphide surface can occur according to:



where n , n_1 and n_2 are the corresponding stoichiometric coefficients, with $n = n_1 + n_2$.

The presence of regions with high concentration of sulphur on the alloy surface after etching, as shown in Fig. 4, supports the formation of this sulphide phase. The pre-treated system can be described by the model depicted in Fig. 10. This model proposes an intermediate Si–O–Al and Al,Cu–S interface and an outermost Si–O–Si rich-film. When time elapses, the aggressive electrolyte penetrates the film structure,

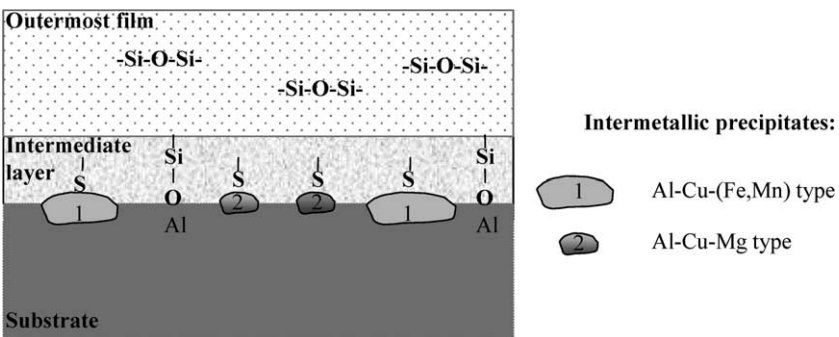


Fig. 10. Schematic illustration of the film/metal interface.

leading to a pronounced decrease of the outermost film resistance and to corrosion onset. After 24 h the time constant at low frequencies is characterised by a capacitance around $20\mu\text{F}/\text{cm}^2$, which is a typical value for a corrosion process controlled by charge transfer.

The electrochemical results show that the pre-treatment with BTESPT leads to improved corrosion resistance of the aluminium based materials. In the case of the AA2024-T3 the pre-treatment confers better protection compared to the Cr reference, for the periods of time studied.

3.3. SKPFM results

SKPFM was used to study the effect of the silane pre-treatment on the potential gradients between the matrix and the intermetallics present in the alloy. Thus, to achieve this objective, i.e., to study the behaviour of the same areas before and after treatment a reference grid was created on the surface, as indicated in Section 2. Figs. 11 and 12 show the SKPFM potential maps and the corresponding profiles obtained in the same area ($40\mu\text{m} \times 40\mu\text{m}$), before and after the silane treatment, respectively. It can be observed that the intermetallic particles, existing in that area exhibit a Volta potential more positive than the matrix. Buchheit [13] has compiled the corrosion potentials in solution of the different phases present in the Al–Cu–(Mg, Fe, Mn, Si) alloy system, which includes AA2024. The measurements indicate the relative nobility of the two main types of particles present in the AA2024-T3. The Al–Cu–(Fe, Mn) particles should be noble relative to the Al matrix, whereas Al–Cu–Mg particles should be active. Frankel et al. [11,12,14] have found that the noble potentials obtained for Al–Cu–(Fe, Mn) in air measurements by SKPFM, are in good agreement with values measured in solution; however, the Al–Cu–Mg also exhibit noble potentials in air, which is in contrast with the active corrosion potentials reported for bulk intermetallic particles in solution. The authors have attributed the highest Volta potential of Al_2CuMg particles measured in air to the presence of a surface film, which composition changed during the polishing steps. In another work [16] the Volta potential gradient between intermetallics and the surrounding matrix was studied on the AA7075-T6 and it was shown that the differences are dependent on the nature of the intermetallics, being strongly affected by the heat treatment.

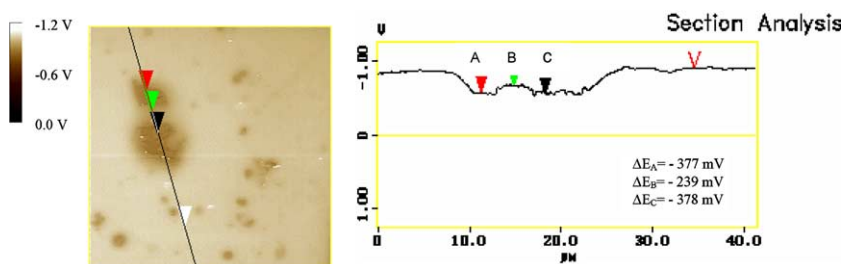


Fig. 11. SKPFM potential map and profile of AA2024-T3 ($40\mu\text{m} \times 40\mu\text{m}$) before silane pre-treatment.

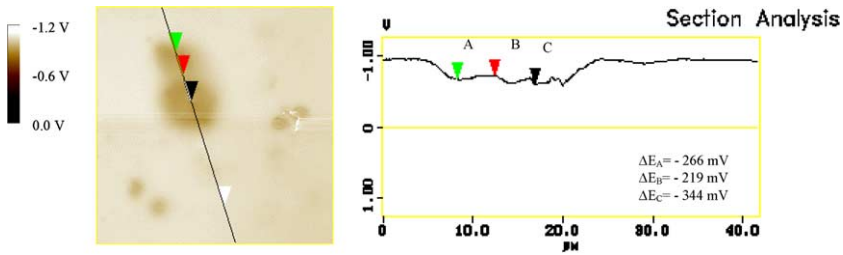


Fig. 12. SKPFM potential map and profile of AA2024-T3 (40 $\mu\text{m} \times 40 \mu\text{m}$) after silane pre-treatment.

Comparing Figs. 11 and 12 it could be seen that the gradient of the Volta potential between the intermetallic particles and the matrix decreases after the silane pre-treatment. This result suggests that the silane pre-treatment seems to induce a modification of the interface metal/film. The existence of copper in the intermetallics, and its high affinity for sulphur, could explain the modification of the interface, by the formation of a thinner sulphide internal layer as also suggested in previous works [3,6,7].

The present work shows that the pre-treatment of the AA2024-T3 results in the formation of a protective surface film. This film seems to be homogeneous, covering the entire surface, including intermetallics and precipitates. Moreover, after film formation there is evidence of chemical changes on the interface associated with the sulphur groups of the silane molecule and the Cu-rich intermetallics present in the alloy.

4. Conclusions

Pre-treatments using the bis-sulphur silane have promising future as chromate replacers on AA2024-T3.

The results show that the silane film provides increased protection to the substrate. At least for short term the performance is even better than that conferred by the chromate reference treatment.

The formation of the silane film on AA2024-T3 may be facilitated by the presence of Cu-rich intermetallics, probably due to the high affinity between copper and sulphur. Thus, the presence of the sulphur on the silane molecule could play an important role on the adherence of the film to the substrate.

References

- [1] G.P. Sundararajan, W.J. van Ooij, *Surf. Eng.* 16 (2000) 315.
- [2] W.J. van Ooij, T.F. Child, *CHEMTEC* 28 (1998) 26.
- [3] W.J. van Ooij, D.Q. Zhu, G. Prasard, S. Jayaseelan, Y. Fu, N. Teredesai, *Surf. Eng.* 16 (2000) 386.
- [4] W.J. van Ooij, D.Q. Zhu, *Proceedings of Corrosion 2000, Orlando (USA)* (2000) 96.
- [5] A.M. Beccaria, L. Chiaruttini, *Corros. Sci.* 41 (1999) 885.
- [6] D. Zhu, W.J. van Ooij, *Corros. Sci.* 45 (2003) 2177.

- [7] W.J. van Ooij, D. Zhu, *Corrosion* 57 (2001) 413.
- [8] W. Yuan, W.J. van Ooij, *J. Colloid Interface Sci.* 185 (1997) 197.
- [9] A. Franquet, C. Le Pen, H. Terryn, J. Vereecken, *Electrochim. Acta* 48 (2003) 1245.
- [10] D. Zhu, W.J. van Ooij, *Corros. Sci.* 45 (2003) 2163.
- [11] P. Schmutz, G.S. Frankel, *J. Electrochem. Soc.* 145 (1998) 2285.
- [12] P. Leblanc, G.S. Frankel, *J. Electrochem. Soc.* 149 (2002) B239.
- [13] R.G. Buchheit, *J. Electrochem. Soc.* 142 (1995) 3994.
- [14] V. Guillaumin, P. Schmutz, G.S. Frankel, *J. Electrochem. Soc.* 148 (2001) B163.
- [15] M.G.S. Ferreira, R.G. Duarte, M.F. Montemor, A.M.P. Simões, *Electrochim. Acta* 49 (2004) 2927.
- [16] F. Andreatta, H. Terryn, J.H.W. de Wit, *Corros. Sci.* 45 (2003) 1733.